Bull Earthquake Eng (2009) 7:701–718
DOI 10.1007/s10518-009-9120-y

ORIGINAL RESEARCH PAPER

An Atlas of ShakeMaps and population exposure catalog for earthquake loss modeling

Trevor I. Allen · David J. Wald · Paul S. Earle · Kristin D. Marano · Alicia J. Hotovec · Kuowan Lin · Michael G. Hearne

Received: 18 December 2008 / Accepted: 25 April 2009 / Published online: 26 May 2009

Abstract We present an Atlas of ShakeMaps and a catalog of human population exposures to moderate-to-strong ground shaking (EXPO-CAT) for recent historical earthquakes (1973–2007). The common purpose of the Atlas and exposure catalog is to calibrate earthquake loss models to be used in the US Geological Survey's Prompt Assessment of Global Earthquakes for Response (PAGER). The full ShakeMap Atlas currently comprises over 5,600 earthquakes from January 1973 through December 2007, with almost 500 of these maps constrained—to varying degrees—by instrumental ground motions, macroseismic intensity data, community internet intensity observations, and published earthquake rupture models. The catalog of human exposures is derived using current PAGER methodologies. Exposure to discrete levels of shaking intensity is obtained by correlating Atlas ShakeMaps with a global population database. Combining this population exposure dataset with historical earthquake loss data, such as PAGER-CAT, provides a useful resource for calibrating loss methodologies against a systematically-derived set of ShakeMap hazard outputs. We illustrate two example uses for EXPO-CAT; (1) simple objective ranking of country vulnerability to earthquakes, and; (2) the influence of time-of-day on earthquake mortality. In general, we observe that countries in similar geographic regions with similar construction practices tend to cluster spatially in terms of relative vulnerability. We also find little quantitative evidence to suggest that time-of-day is a significant factor in earthquake mortality. Moreover, earthquake mortality appears to be more systematically linked to the population exposed to severe ground shaking (Modified Mercalli Intensity VIII+). Finally, equipped with the full Atlas of ShakeMaps, we merge each of these maps and find the maximum estimated peak ground acceleration at any grid point in the world for the past 35 years. We subsequently compare this "composite

T. I. Allen and M. G. Hearne—contracted through Synergetics Incorporated.

T. I. Allen · D. J. Wald · P. S. Earle · K. D. Marano · A. J. Hotovec · K. Lin · M. G. Hearne
National Earthquake Information Center, US Geological Survey, Golden, CO, USA

Present Address:
T. I. Allen (✉)
Risk and Impact Analysis Group, Geoscience Australia, Canberra, Australia
e-mail: trevor.allen@ga.gov.au

ShakeMap" with existing global hazard models, calculating the spatial area of the existing hazard maps exceeded by the combined ShakeMap ground motions. In general, these analyses suggest that existing global, and regional, hazard maps tend to overestimate hazard. Both the Atlas of ShakeMaps and EXPO-CAT have many potential uses for examining earthquake risk and epidemiology. All of the datasets discussed herein are available for download on the PAGER Web page (http://earthquake.usgs.gov/eqcenter/pager/prodandref/).

Keywords ShakeMap Atlas · PAGER · Loss modeling · Hazard · Risk · Time-of-day

1 Introduction

Several recent publications (e.g., Bilham 2004; Ramirez and Peek-Asa 2005; Jackson 2006; Spence 2007) warn of the seismic risk to growing global communities, particularly in the developing world where earthquake resistant design and construction are not commonly practiced or stringently enforced. A poignant reminder of this was the May 12, 2008 M_W 7.9 Wenchuan, China earthquake. The event killed in excess of 69,000 people (World Health Organization 2008) in a region with arguably better construction practices than other regions of the developing world. With this in mind, it is important that emergency managers and responders be prepared for catastrophic impacts of future earthquakes in modern society. Mortality rates are often dependent on the timely dispatch of search and rescue teams to an affected region (Macintyre et al. 2006). The development of robust loss models using the data presented herein represents an important first step in being able to rapidly assess the impact of any global earthquake within minutes-to-hours of its occurrence. Tools such as PAGER (Prompt Assessment of Global Earthquakes for Response, Earle et al. 2008; Wald et al. 2008a), which rapidly estimate the number of people exposed to moderate-to-strong levels of shaking, could greatly reduce response times and assist emergency managers in evaluating the appropriate response, thereby potentially saving lives.

A natural progression from providing information regarding the number of people exposed to significant levels of ground shaking is to provide an estimate of the number of potential fatalities. In order to develop global loss models for rapid impact assessment of earthquakes, we required the development of a catalog of human population exposures, EXPO-CAT, from recent historical earthquakes (since 1973). PAGER will employ these models to rapidly estimate the impact of global earthquakes as part of the US Geological Survey (USGS) National Earthquake Information Center's earthquake response protocol.

EXPO-CAT is derived from two key datasets: the PAGER-CAT earthquake catalog (Allen et al. 2009) and the Atlas of ShakeMaps (Allen et al. 2008). PAGER-CAT provides accurate earthquake source (e.g., hypocenter and magnitude) information necessary to compute reliable ShakeMaps (e.g., Wald et al. 1999b, 2005) in the Atlas. It also contributes loss information (i.e., number of deaths and injuries) from historical events. The Atlas of ShakeMaps, on the other hand, provides us with the shaking distribution for over 5,600 earthquakes from which we estimate the number of people exposed to different levels of shaking intensity.

The catalogs and databases discussed herein provide an essential resource for the development of global earthquake fatality and loss models. Though developed primarily for the PAGER project, we anticipate other uses for these datasets, including the provision of information for disaster response, scenario planning, mitigation, and outreach programs. The dataset will also facilitate the calibration of rapid landslide (Godt et al. 2008) and liquefaction assessments following large earthquakes, and subsequent estimation of the potential

impact from these secondary hazards (e.g., Marano et al. 2009). Data from the ShakeMap Atlas and EXPO-CAT could also facilitate direct comparison of loss estimates for alternative loss methodologies against a systematically-derived set of ShakeMap hazard outputs.

2 PAGER-CAT earthquake catalog

PAGER-CAT forms the basis for the development of both the Atlas of ShakeMaps and EXPO-CAT. It was developed by combining high-quality earthquake source and loss information from several global earthquake catalogs (Allen et al. 2009). A key priority in developing the catalog was to provide consistently derived technical information for global earthquakes from recognized data centers and researchers. The high-quality earthquake hypocenters and magnitudes indicated in PAGER-CAT are necessary for the calculation of individual ShakeMaps in the Atlas of ShakeMaps.

PAGER-CAT incorporates eight global earthquake catalogs and additional auxiliary data to provide accurate information, not only for hypocentral locations, magnitudes and human casualties, but also detailed focal mechanism information, the country of origin, local time and day of week. Where available, an indication of secondary effects (e.g., tsunami, landslide, fire or liquefaction) and deaths attributed to these effects (Marano et al. 2009), the number of buildings damaged or destroyed, and the number of people injured or left homeless are also provided. The present version of the catalog comprises over 140 fields in which detailed event information can be recorded and currently includes over 22,000 events from January 1900 through December 2007, with an emphasis on earthquakes since 1973. We use 1973 as a cut-off date for our work because this is the official start date of one of our primary data sources for earthquake origins and casualties; the USGS's Preliminary Determination of Epicenters. PAGER-CAT indicates 1,373 earthquakes since 1900 with at least one reported fatality. PAGER-CAT is a composite earthquake catalog that has been developed entirely from published or online databases and reports. No new information has been derived in its compilation. However, for the first time, it aggregates the most authoritative information from a range of sources into a comprehensive, easy to use digital format that is publically available.

Regularly updated versions of PAGER-CAT will be available at: http://earthquake.usgs.gov/research/data/pager/. The catalog is available for download as a comma-delimited text file, which can be imported into geographical information systems such as ESRI ArcGIS™, or as a Matlab™ data file that can be queried with an accompanying function. We encourage contributions and corrections from the community to further improve the catalog for all interested users. Updates can be made directly to a condensed version of PAGER-CAT available on Wikipedia (http://en.wikipedia.org/wiki/List_of_deadly_earthquakes_since_1900). More detailed contributions should be forwarded to the authors for inclusion in subsequent catalog releases.

3 Atlas of global ShakeMaps

Maps of peak ground motions (PGA and PGV) and intensity have been calculated for some 5,650 recent historical (1973–2007) global earthquakes. The processes for choosing events included in the Atlas are described further in Allen et al. (2008). However, a minimum requirement is that the earthquakes have a magnitude of M_W 5.5 or greater (M_W 4.5 in stable continental regions) and resulted in approximately 3,000 people being exposed to Modified

Mercalli Intensity (MMI) VI or greater. Additionally, earthquakes are included if they are reported to have had human casualties (fatalities or injuries).

The Atlas was produced using established ShakeMap methodology (Wald et al. 1999b, 2005) and constraints from macroseismic intensity data, instrumental ground motions, regional topographically-based site amplifications (Wald and Allen 2007), and published earthquake source dimensions. The Atlas uses high-quality locations, coupled with moment magnitudes from PAGER-CAT. Applying the ShakeMap methodology allows a consistent approach to combining point ground shaking observations with ground motion predictions to produce an estimated spatial shaking distribution for each event. Along with the standard ShakeMap outputs (e.g., peak acceleration, velocity and instrumental intensity), we also calculate an estimated ground motion uncertainty at each grid point (Wald et al. 2008b). Since the science, data availability, and further earthquake studies continue to improve our capacity to estimate shaking for earthquakes in the Atlas, we expect to update many or all events in the Atlas on an occasional basis as these advancements become available. The online Atlas and supporting databases can be found at: http://earthquake.usgs.gov/eqcenter/shakemap/atlas/.

4 EXPO-CAT human exposure catalog

Using historical earthquakes in the Atlas of ShakeMaps and a gridded global population database, we obtain an estimate of the number of people exposed to discrete levels of instrumental intensity (Wald et al. 1999a). Present-day exposure is estimated using the Oak Ridge Laboratory's Landscan 2006 global population database (e.g., Dobson et al. 2000; Bhaduri et al. 2002). We subsequently hindcast these numbers to the date of the earthquake using United Nations national population growth rate data (United Nations 2006). These growth rates ignore changes in demographics within a country, including the growing disparity in growth between urban and rural regions over recent decades. This is another of the key reasons for limiting both the Atlas of ShakeMaps and EXPO-CAT to post-1973 earthquakes because global growth rate information becomes less reliable for time periods prior to this, and it becomes more difficult to estimate pre-earthquake population exposure. We use the following exponential equation to hindcast the population exposure E_{h} for each intensity level from present-day (i.e., from LandScan 2006) population E_{p};

$$E_{\mathrm{h}} = E_{\mathrm{p}}/(1+r)^{T} \tag{1}$$

where r is the national growth rate and T is the time lapse (in years) between the event and mid-2006.

Since the instrumental intensity estimates that are calculated in ShakeMap are floating point values, we extract population exposures in half-intensity unit bins. Hindcasted population estimates for each ShakeMap are aggregated into EXPO-CAT, in addition to the growth rate r used to depreciate population numbers. The total population exposure for each earthquake is separated between urban and rural settings for each intensity level using the Global Rural-Urban Mapping Project extents (Center for International Earth Science Information Network 2005). However, the example uses of EXPO-CAT outlined below use total population exposure only. EXPO-CAT also includes ShakeMap parameters such as the preferred earthquake source parameters (Allen et al. 2009), the ground motion prediction equation used, and shaking uncertainty factor (Wald et al. 2008b). EXPO-CAT is subsequently combined with PAGER-CAT to provide earthquake loss information and country of origin, in addition to information regarding the occurrence of secondary earthquake impacts, such as

landslides, tsunami and fire, which may have also contributed to losses (Allen et al. 2009). More detailed information on the content of EXPO-CAT can be found at: http://earthquake.usgs.gov/research/data/pager/expocat/.

5 Uses of EXPO-CAT

The primary reason for the development of EXPO-CAT is to support the development of earthquake loss models. These methodologies are discussed in recent (Jaiswal and Wald 2008; Porter et al. 2008b) and forthcoming publications (K. S. Jaiswal and K. A. Porter, personal commununication). The combination of EXPO-CAT with earthquake casualty databases, such as PAGER-CAT, allows us to investigate, or revisit, a wide range of factors affecting the occurrence, relative impact, and epidemiology of earthquakes. For illustration, we use EXPO-CAT to derive country-specific earthquake vulnerability rankings, and assess the effect of time-of-day on mortality rates.

5.1 Ranking of country earthquake vulnerability

Intuitively we know that the vulnerability of global communities varies from country-to-country, or even between urban and rural communities within a country. For example, building code-based engineered structures are more likely to resist failure under strong ground shaking than informally constructed structures, such as those common in the developing world (Jaiswal and Wald 2008). Using EXPO-CAT, we have formulated a simple, yet objective, vulnerability ranking scheme for countries where earthquake fatalities have been documented around the globe. In developing global fatality models, it is useful to rank and group countries of similar construction practice and vulnerability, particularly where we have little information to constrain country-specific loss models.

We apply a simple a priori fatality model as a function of shaking intensity to hindcasted population exposure estimates and apply to all global earthquakes in EXPO-CAT. The fatality model was derived for all global data using the Nelder–Mead technique (The MathWorks 2008), minimizing a logarithmic objective function (e.g., The MathWorks 2008), and has the form;

$$R(I) = 10^{(1.03I - 10.75)} \tag{2}$$

where R is the fatality rate (fatalities per number of people exposed) at intensity I (Fig. 1). Ratios of the observed and predicted fatality values are grouped by country and averaged. The countries are subsequently ranked by this average ratio. The resulting plot (Fig. 2) indicates a relative morbidity ranking for countries that have experienced at least two or more earthquakes with 10 or more shaking related fatalities (i.e., from partial or total building collapse) since 1973. We make the assumption that this relative morbidity ranking can be mapped directly to structural vulnerability because the chief cause of death in earthquakes is through partial or total building collapse. Spatial examination of these rankings indicate that countries in different geographic regions appear to cluster spatially according to their relative vulnerability (Fig. 3). Thus, this ranking scheme could be used to guide country groupings where little data exist to generate country-specific loss models. The ranking could also be extended to neighboring countries in a geographical region where no data exist to provide an empirically based ranking.

These vulnerability rankings should only be used as a simple guide because large inter-event variability between earthquakes could lead to unwarranted vulnerability clas-

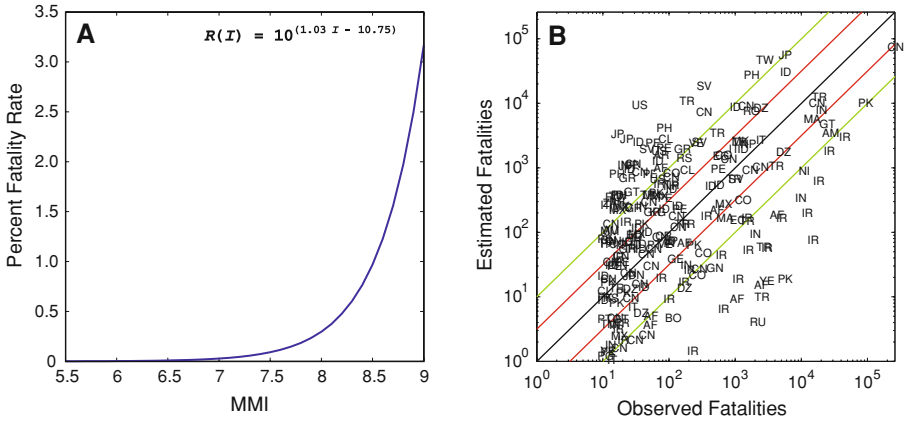

Fig. 1 A priori fatality model used to approximate and rank the seismic vulnerability of countries around the world. **a** The first-order fatality curve is based on global data and relates the percentage of fatalities to the number of people exposed at different MMI levels. **b** Observed verses predicted fatalities for all global earthquakes with shaking-related deaths of ten or more. The approximate lognormal distribution of the data suggests this model serves as a reasonable proxy to rank global earthquake vulnerabilities. Each data point is labeled with a two letter International Organization for Standardization (ISO) country code (ISO 2007). The *green* and *red lines* indicate one and one-half orders of magnitude uncertainty bounds, respectively

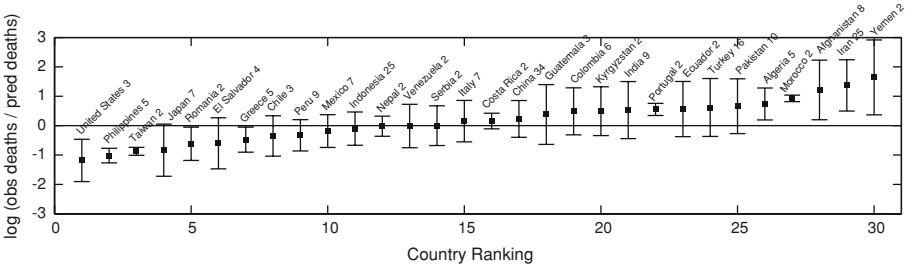

Fig. 2 Ratios of observed and predicted fatalities, averaged for each country, and ranked by apparent vulnerability. Only countries that have experienced more than one earthquake resulting in ten or more shaking deaths (i.e., from partial of total building collapse) are indicated. The number of earthquakes used to calculate the rankings are indicated after the country name. It is important to note that these vulnerability rankings should not be considered absolute. The rankings provided are based purely on empirical analysis of historical earthquake data and the estimated population exposed to different levels of ground shaking. These rankings should be combined with expert opinion to ascertain more rigorous rankings that consider construction type and its likely response to strong ground shaking

sifications for some countries. Consequently, these results should be combined with expert opinion to ascertain more reliable rankings that consider construction type and its likely response to strong ground shaking. For example, the apparent low vulnerability of Romania is largely driven by the high intensities assigned in post-disaster surveys from the 1977 M_W 7.5 Vrancea earthquake (e.g., Radu et al. 1979). These intensities have been incorporated into the Atlas of ShakeMaps in an effort to replicate observed shaking for this event (see http://earthquake.usgs.gov/eqcenter/shakemap/atlas/shake/1977030419 21/). This possible overestimation of intensity over a large spatial area for the Vrancea earthquake subsequently increases the number of people and structures exposed to severe ground-shaking, which acts to lower the relative vulnerability ranking.

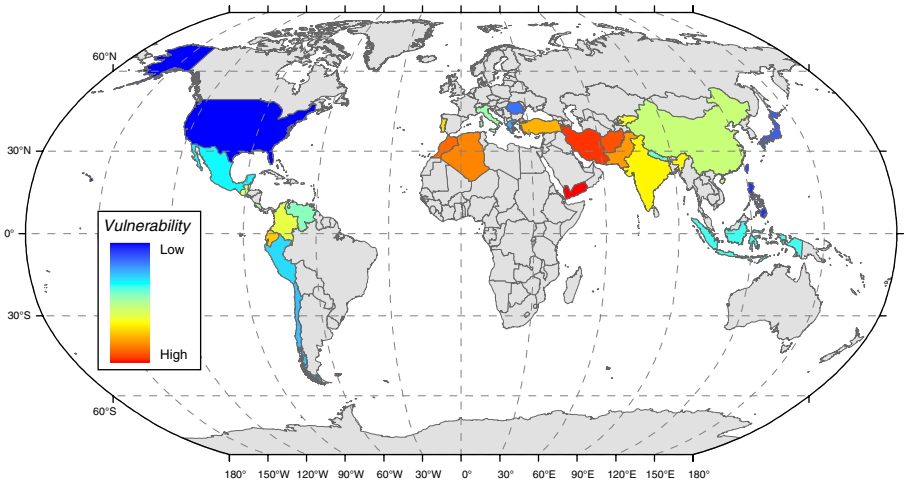

Fig. 3 Spatial representation of the global earthquake vulnerability rankings in Fig. 2. Countries *shaded with grey* have not experienced two or more earthquakes where ten or more people have perished since 1973, and thus were not considered in this analysis. As discussed in the Fig. 2 caption, these rankings should not be considered absolute and are based purely on empirical analysis of historical earthquake data and the estimated population exposed to different levels of ground shaking. However, in general, the rankings appear to be consistent with what is known about global construction practices (e.g., Jaiswal and Wald 2008)

In contrast, if we were to reduce the number of events per country required for our relative vulnerability ranking assessment to one or more earthquakes (rather than two or more), we would have observed Russia as being the most vulnerable country to earthquakes. This apparent high vulnerability of Russia is due to one earthquake: the 1995 M_W 7.0 Sakhalin Island (eastern Russia) earthquake in which almost 2,000 people perished in the town of Neftegorsk, which had a pre-earthquake population of about 3,000 (Johnson 1998). This town was not reoccupied after the quake, which subsequently leads to an underestimate of population exposure for the 1995 earthquake from hindcasting the present-day population distribution. To a first order, the country rankings indicated in Fig. 2 are consistent with what is known about the vulnerability of the global building stock (e.g., Jaiswal and Wald 2008; Porter et al. 2008b). However, the examples of Romania and Russia demonstrate the perils in estimating population exposure for historical earthquakes, particularly when there is uncertainty associated with historical shaking estimates or population distributions. Another notable outlier includes Nepal. The ranking of Nepal was based on few earthquakes, none of which possessed calibration information from which to estimate the ground shaking distribution.

It should also be considered that differences in structural vulnerability can also exist within a given country due to climatic, social, cultural or economic inhomogeneities. This, for example, is true of the eastern and western United States (e.g., Building Seismic Safety Council 2004), and ideally these differences should also be considered.

Time-of-day analyses

Several authors suggest that time-of-day may have a bearing on the human impact observed following large earthquakes (e.g., Lomnitz 1970; Scawthorn 1978; Coburn et al. 1992; Ramirez and Peek-Asa 2005; Tierney et al. 2005), with night-time earthquakes, particularly in the developing world, generally considered to be the most deadly. This assumption has largely been based on the fact that some of the world's deadliest earthquakes have indeed

Table 1 List of earthquakes resulting in more than 10,000 fatalities from partial or total building collapse since 1970 (Source Allen et al. (2009) and World Health Organization 2008)

Date (UTC)	Local time	Earthquake location	Moment magnitude	Killed	Injured
1970-01-04	1:00	Tonghai, China	7.2	15,621	26,783
1972-12-23	0:29	Managua, Nicaragua	(M_S) 6.2	11,000	20,000
1976-02-04	3:01	Guatemala	7.5	22,778	76,504
1976-07-27	3:42	Tangshan, China	7.6	242,419[a]	164,581
1978-09-16	19:05	Tabas, Iran	7.4	18,220	–
1988-12-07	11:41	Spitak, Armenia	6.7	25,000	20,000
1990-06-20	0:30	Manjil, Iran	7.4	45,000	60,000
1999-08-17	2:01	Kocaeli, Turkey	7.6	17,439	43,953
2001-01-26	8:46	Bhuj, India	7.6	20,023	166,836
2003-12-26	5:26	Bam, Iran	6.6	26,271	30,000
2005-10-08	8:50	Kashmir, Pakistan	7.6	87,351	75,266
2008-05-12	14:28	Wenchuan, China	7.9	69,195[b]	374,176[b]

Local time is indicated as 24 h time
[a] Official death toll. Unofficial death toll is 655,237 (e.g., Spence 2007)
[b] Approximate toll as of July, 2008 (World Health Organization 2008)

occurred in the early morning hours where it is assumed that victims; (1) are occupying unsafe dwellings, and (2) are not alert and are unable to escape their dwellings during the earthquake. However, there has been very little quantitative evidence provided to support this theory. Table 1 provides a list of the world's deadliest earthquakes since 1970, where fatalities are largely attributed to partial or total structural collapse rather than secondary effects (e.g., landslides, tsunami, fire, etc.). As observed in Table 1, many of these events have occurred in the early hours of the morning. But is this simply a result of the highest exposure earthquakes occurring during these early morning hours? We use our catalog of human exposures to examine this question.

A list of countries that currently observe daylight savings was obtained from the website http://timeanddate.com, and events occurring in these regions were flagged. For earthquakes occurring in countries that observe daylight savings, a correction of 1 h was applied for the months April through September in the northern hemisphere, and October through March in the southern hemisphere. We acknowledge that the observation of daylight savings in some countries may have varied since 1973, and that there are even regional differences within a country. Consequently, we make no attempt to justify that our daylight saving correction is absolute. However, it does provide an improved correction factor to local time-of-day which otherwise would not be considered. Moreover, it is generally observed that most developing nations (those most vulnerable to earthquakes) do not observe daylight savings, and as such, this correction factor does not apply.

Using only fatal earthquakes in the global exposure catalog (since 1973), we aggregate the number of deaths to have occurred from earthquake shaking for each local hour and find its percentage of total shaking deaths over the full 24 h of the day (Fig. 4a). In this step we limit the maximum number shaking deaths to 50,000. This is so the 1976 Tangshan, China (local time 3:42 a.m.) and 2005 Kashmir, Pakistan (local time 8:50 a.m.) earthquakes do not dominate global or regional results. If time-of-day is a significant factor, it should still emerge in the absence of these events. From Fig. 4a, it does appear that earthquakes occurring in the early morning hours do tend to dominate the number of fatalities observed

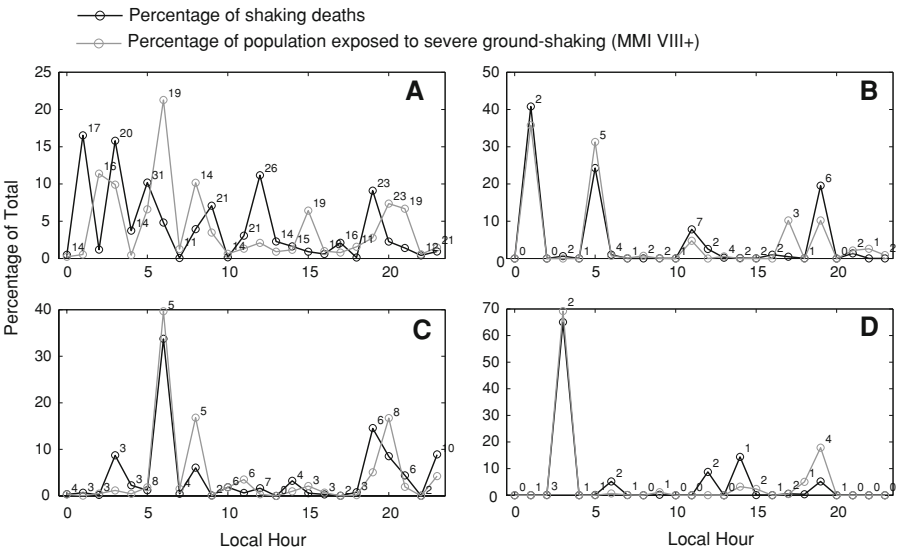

Fig. 4 Percentage of shaking deaths to have occurred at each local hour, in addition to the estimated percentage of people exposed to MMI VIII and higher for; **a** all global earthquakes since 1973 with shaking fatalities; **b** the Middle East (Afghanistan, Iran, Iraq and Yemen); **c** Eastern Asia (China and Indonesia) and; **d** Turkey. *Numbers* to the *top-right* of data points represent the number of events in that hour window

from earthquake shaking globally. We perform equivalent analyses for population exposure, thus finding the hourly percentage of exposure to severe ground-shaking (Fig. 4a). Herein, we define severe shaking intensity as MMI VIII and above. This plot does, to some extent, indicate similar trends to the fatality plot. However, population exposure appears to be more uniformly distributed across the full 24 h of the day, suggesting that there may be a small time-of-day effect using all global data.

The prior analyses using the full global dataset may lead to erroneous conclusions since a country with high vulnerability may dominate the number of deaths and have relatively sparse exposure (e.g., Iran), while a country that has many seismically resistant structures and high population density may dominate the exposure (e.g., Japan) for any particular hour. Consequently, we have grouped countries that have similar perceived vulnerability and geographic region based on our simple vulnerability rankings discussed above. We have also ensured that these groupings have abundant loss data. Similar analyses to that of the global dataset are performed for the Middle East (Afghanistan, Iran, Iraq, and Yemen), eastern Asia (China and Indonesia), and Turkey. In the Middle Eastern region (Fig. 4b), we do see evidence to suggest that earthquakes in the early morning hours may contribute more to the observed losses. However, there is also a strong correlation to the number of people exposed to severe shaking. While we accept that there could be significant uncertainties in our exposure numbers from the estimated shaking distribution and hindcasted exposure from present-day population, we see no strong evidence to suggest that time-of-day is a factor in the mortality rates observed in the Middle East. In the eastern Asian region, deaths and exposure are again well correlated, with the 2006 Yogyakarta, Indonesia earthquake dominating the fatalities and exposure (Fig. 4c). Finally, earthquake fatalities in Turkey are dominated by the 1999 Kocaeli earthquake, which occurred in the third hour of the local day (Fig. 4d). Again, the percentage of total population exposure to severe ground-shaking is well-correlated to the percentage of total fatalities for this hour. Although this analysis is not exhaustive and

there may be uncertainties associated with our estimates of ground shaking and subsequent population exposure, there appears to be little empirical evidence linking earthquake-related fatalities to time-of-day for many global regions. It is important to note that we do not rule out the time-of-day effect completely, and in some earthquakes it may have contributed to higher rates of earthquake mortality, particularly in the developing world. However, our empirical analysis suggests that this effect may not be as dominant as commonly thought. Moreover, the number of people exposed to severe ground-shaking appears to be a more appropriate indicator of potential earthquake fatalities. These results further demonstrate the importance of rapid assessment and dissemination of post-disaster information regarding the number of people exposed to future earthquakes through tools such as PAGER.

6 Composite global ShakeMap

Armed with over 5,600 ShakeMaps of significant earthquakes, we have created a composite ShakeMap to provide a global perspective of earthquake ground shaking from January 1973 through December 2007. The ShakeMaps are combined to give the estimated maximum peak ground acceleration (PGA) experienced at any grid point (Fig. 5). This map is compared directly to the Global Seismic Hazard Map (GSHAP) of Giardini et al. (1999). While both the Atlas-based and GSHAP maps were derived with a similar catalogue of historical seismicity prior to 1999, the Atlas represents estimated PGA due to events that have actually occurred since 1973 (35 years) and is not influenced by earthquake recurrence estimates, tectonic strain rates, palaeoseismological or geomorphological investigations, or geodetic constraints. Additionally, unlike the GSHAP map, the Atlas-based map was produced with a uniform approach to ground-motion estimation, includes observed ground-shaking data and additional source constraints, and also incorporates amplification from topographically-based seismic site conditions. In contrast, GSHAP used regionally specific approaches to characterize the hazards from region-to-region.

Acknowledging these differences, we are able to compare the two maps. We do this by finding the ratio of the GSHAP map of 10% probability of exceedance in 50 years relative to the composite ShakeMap of PGA. We interpret these probabilities to imply that in a 50 year period, we would expect that 10% of the global landmass will experience PGA equivalent to, or exceeding the hazard values mapped in GSHAP. Given that the ShakeMap Atlas represents 35 years of global ground shaking, we might expect 7% of the global landmass to have exceeded the GSHAP hazard in our time-period of interest. Oceanic areas that have ground-motions and hazard associated with them are masked from the comparisons. There are some important conditions that must be recognized prior to evaluating these results. Because the Atlas was fundamentally designed to support the development of loss estimation methodologies, we only include earthquakes that had significant population exposure to moderate-to-severe levels of ground shaking. Furthermore, we only include earthquakes of magnitude 5.5 and greater (magnitude 4.5 in stable continental regions), unless the earthquake resulted in fatalities (Allen et al. 2008). These factors may lead to an underestimation in the observed PGA in some regions that have only experienced small, non-damaging earthquakes since 1973 (for example, eastern North America). Consequently, the total area of our composite map to have exceeded the assigned PGA hazard in GSHAP should be a slight underestimate of global hazard (that is, less than 7%), since we do not consider full global coverage or lower magnitude events. Another important consideration is that our composite ShakeMap includes the effects of uniform global site response (Wald and Allen 2007), whereas the GSHAP hazard map provides bedrock hazard only. This effect should act to slightly increase

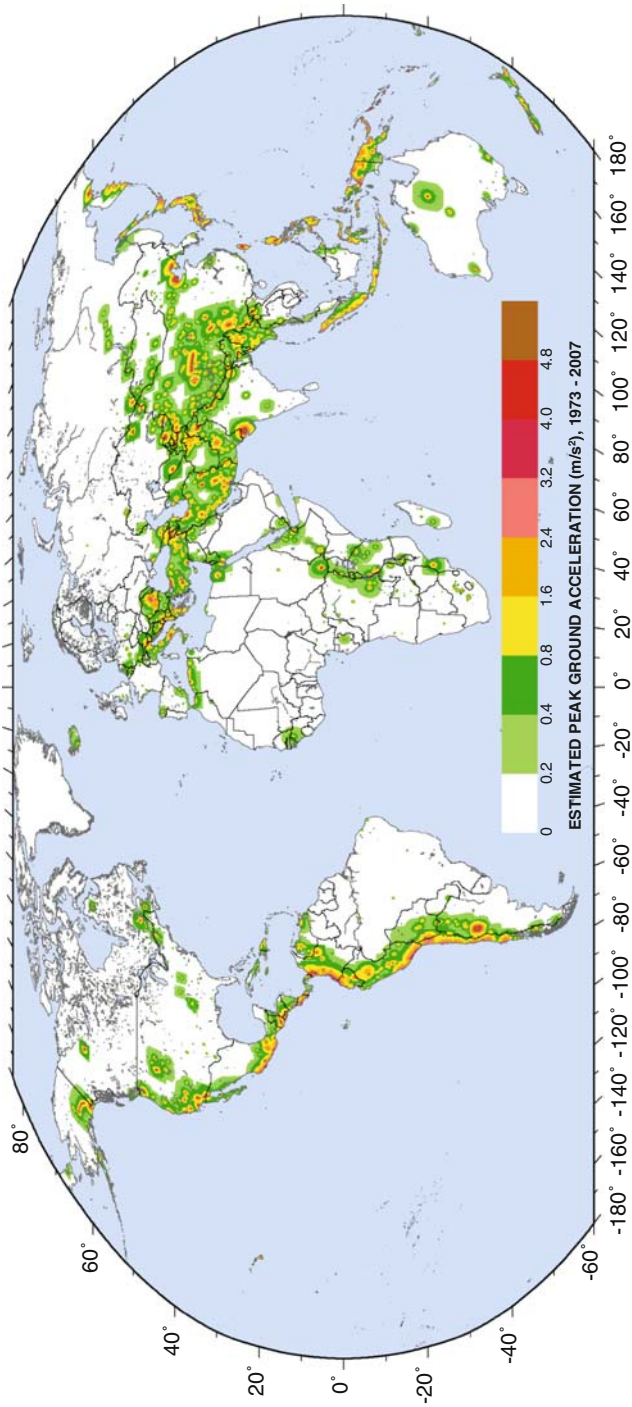

Fig. 5 Composite ShakeMap Atlas indicating the maximum PGA estimated at any location in the World (near significant population exposure) for earthquakes $M_W \geq 5.5$ ($M_W \geq 4.5$ in stable continental regions) from 1973 through December 2007

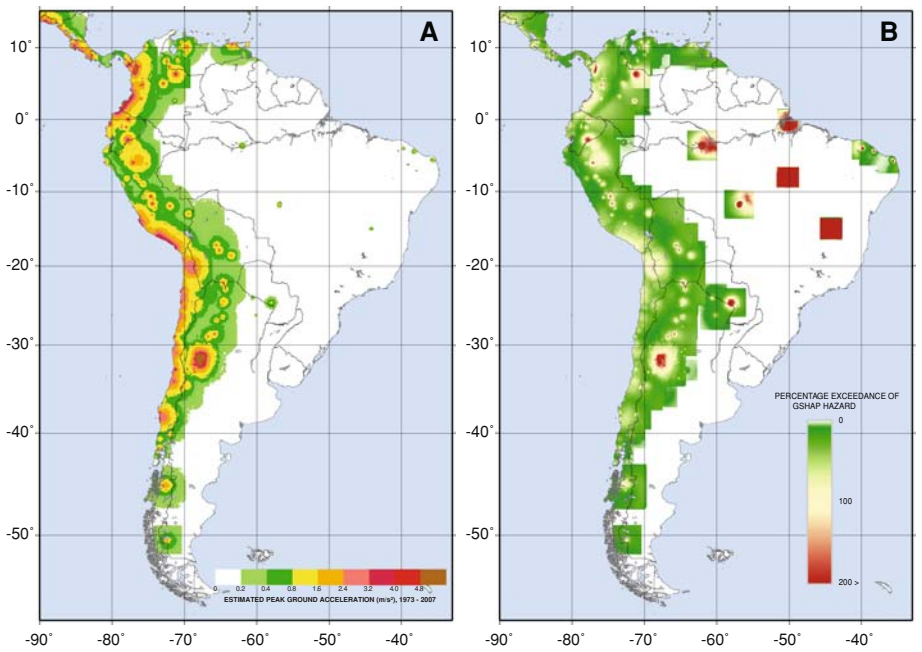

Fig. 6 **a** Combined PGA of Atlas ShakeMaps for South America, and **b** the percentage exceedance of the estimated PGA from 1973 through December 2007 relative to the GSHAP 10% in 50 years hazard map for South America. Values greater than 100% represent regions where GSHAP PGA has been exceeded

the predicted ground-motion, and subsequently, the spatial area on the composite ShakeMap exceeding GSHAP hazard.

Figure 6 indicates the estimated ground-shaking and the percentage exceedance of our composite PGA ShakeMap against the GSHAP map for South America. Percentages lower than, equal to, or above 100% represent where the composite map is lower than, equal to, or exceeds the GSHAP map, respectively. Table 2 summarizes the percentage area of landmass where the composite ShakeMap has exceeded GSHAP hazard for map regions compiled by Grünthal et al. (1999); McCue (1999); Shedlock and Tanner (1999), and Zhang et al. (1999). Other key regions that are well constrained in the Atlas are considered separately (for example, California, Japan and Turkey). We do not attempt to make any qualitative assessments on these results. However, we do note that predicted hazard in most regions appears to be conservative relative to observed seismicity over the past 35 years (for example, Australia, SW Pacific and SE Asia, and the Americas). A possible explanation may be that some probability of large earthquakes occurring was factored into hazard calculations and these events have not been observed in modern times. Note, that the 2004 M_W 9.0 Sumatra-Andaman Islands earthquake and tsunami only affected a small fraction of the landmass in the Australia, SW Pacific and SE Asia hazard map (McCue 1999) in terms of actual ground shaking. Consequently it had only a minor effect on the spatial area of the map that exceeded GSHAP.

In some regions, PGA values from the composite ShakeMap do appear to reflect a percentage area exceeding GSHAP near 7% (for example, Africa and Continental Asia), but anomalies in the mapping of GSHAP hazard may be equally responsible for these "expected" levels of exceedance. We note that sharp transitions—from high-to-low hazard—exist on

Table 2 Percentage of landmass for which the estimated PGA from the composite ShakeMap exceeds the GSHAP 10% chance of exceedance in 50 years hazard map for different regions in the world from January 1973 through December 2007

Region	Map bounds (lon1/lon2/lat1/lat2)	Percent of landmass area exceeded (GSHAP PGA $\geq$ 0.0m/s^2)	Percent of landmass area exceeded (GSHAP PGA $\geq$ 0.8m/s^2)
Africa	–20/55/–36/38	7.3	3.8
Australia	112/155/–45/–10	0.5	1.2
Australia, SW Pacific and SE Asia	93/180/–48/20	2.5	3.7
California and Nevada	–124.5/–114/32.5/42.05	2.2	2.4
Conterminous United States and Mexico	–126/–63/15/50	2.4	2.8
Continental Asia	60/150/0/60	6.4	3.8
Europe	–10/45/35/56	4.6	4.6
Japan	128/146/30/46	8.5	12.6
North America	–180/–30/15/72	1.5	1.9
South America	–90/–33/–57/15	3.4	2.9
Turkey	25.67/44.82/35.81/42.10	4.1	2.8
Global average	–180/180/–60/84	3.8	3.1

Given the composite ShakeMap represents 35 years of global ground shaking, we might expect 7% of the landmass to have exceeded GSHAP. Exceedance percentages of PGA hazard are indicated for all regions regardless of the GSHAP hazard, and also for the limited spatial areas where GSHAP predicts PGA hazard $\geq$0.8 m/s^2

the GSHAP map rather than smoothly varying hazard values. Consequently, moderate-sized earthquakes near these boundaries may exceed the hazard on one side of a seismic source zone, but not on the other. This is particularly apparent for the African (Fig. 7) and continental Asia (not shown) maps and results in relatively minor ground motions contributing to the areal extent of exceedance in background seismic source zones. To mitigate this effect, we perform the same analyses as above, but only consider onshore regions where GSHAP maps PGA hazard at 0.8 m/s^2 and higher. In general, we observe that the estimated level of exceedance for Africa and Continental Asia reduces to become more consistent with other global regions. Overall, the GSHAP seismic hazard map appears to overestimate global hazard when compared to our composite ShakeMap of estimated observed PGA since 1973. The one exception is Japan, which has an estimated area of exceedance at 12.8% for areas of GSHAP PGA $\geq$ 0.8 m/s^2. Japan is one region where we have an abundance of instrumental ground-motion data and finite fault models to constrain the ShakeMaps in the Atlas that make up the composite ShakeMap. Consequently, we are confident that its representation of maximum PGA is reliable. Little information is provided in Zhang et al. (1999) as to how the GSHAP hazard map for Japan was developed, and we are still unclear about the discrepancies observed between our composite ShakeMap and the predicted GSHAP PGA hazard for Japan.

The very low area of exceedance observed for the US comparisons are commensurate with the overall reduction in hazard predicted by the new US National Seismic Hazard Maps (Petersen et al. 2008). However, we have not attempted a direct comparison to these new hazard maps.

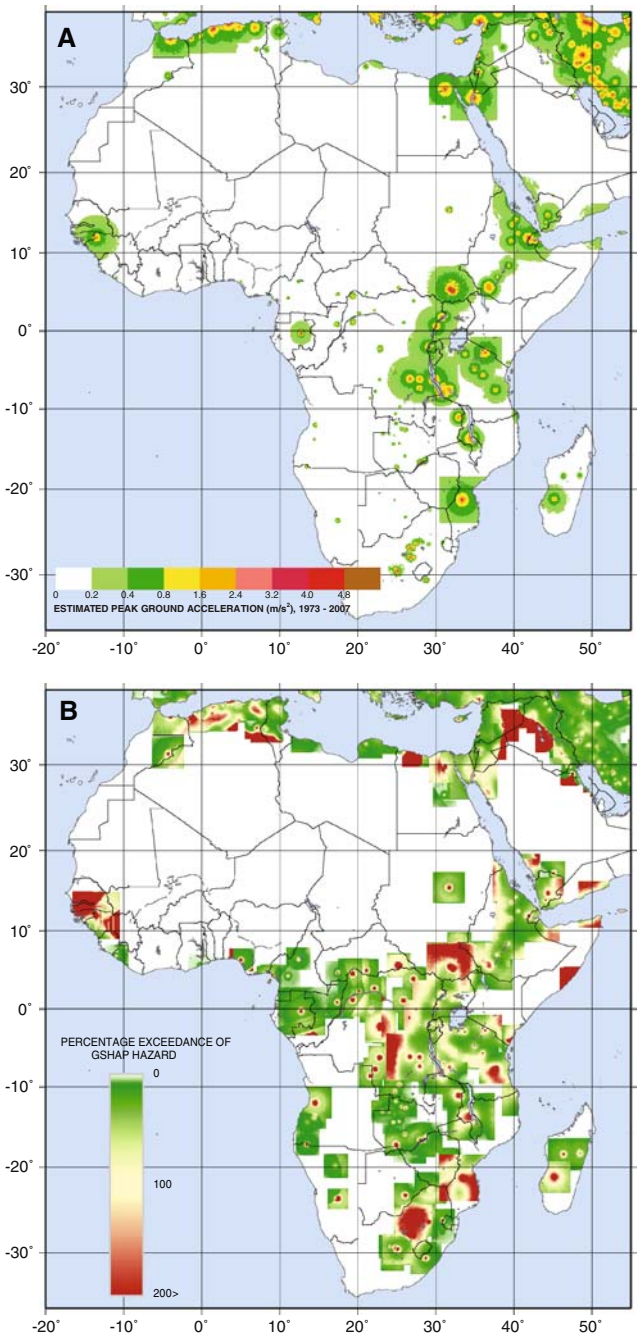

Fig. 7 **a** Combined PGA of Atlas ShakeMaps for Africa, and **b** the percentage exceedance of the estimated PGA from 1973 through December 2007 relative to the GSHAP 10% in 50 years hazard map for Africa. Values greater than 100% represent regions where GSHAP PGA has been exceeded. Note that sharp transitions from high-to-low hazard exist on the GSHAP map rather than smoothly varying hazard values. Consequently, moderate-sized earthquakes near these boundaries exceed the hazard on one side of the boundary, but not on the other

Because there are many events within the Atlas that have no data constraints, we acknowledge that there may be some uncertainty associated with purely predictive ground-motions. We also note potential problems with ground motion equations in predicting ground motions beyond the distance range in which they were defined (e.g., 100–200 km for some models), and this is the focus of ongoing research (Allen and Wald 2009). However, many of the largest events in the catalogue that exceed GSHAP hazard are indeed well-constrained with finite-fault models and some information regarding the level of ground shaking, whether it be from instrumental or macroseismic ground motions.

It is important to note that the composite ShakeMap should not be used as a replacement for traditional seismic hazard maps. This is because the composite ShakeMap does not include hazard from background seismic sources. Furthermore, it does not sample all global regions that may be of strategic importance for the planning and development of major infrastructure, such as nuclear or toxic waste facilities, and oil and gas pipelines. For example, the 1986 M_W 5.7 Marryat Creek earthquake (Machette et al. 1993) occurred in a sparsely populated region of central Australia and thus did not meet the population threshold required for inclusion into the Atlas. However, the surface rupture and ground motions produced from this quake, and others like it, would still be critical to consider in the placement and seismic design of such installations. Though the composite ShakeMap is not sufficient to evaluate global hazard itself, it does provide a useful guide as to whether hazard maps, such as GSHAP, offer a realistic interpretation of global seismic hazard in high-exposure, high-risk regions.

7 Discussion and conclusions

An Atlas of some 5,650 ShakeMaps has been produced using established ShakeMap methodology and constraints from macroseismic intensity data, instrumental ground motions, regional topographically-based site amplifications, and published fault rupture dimensions. Though developed primarily for PAGER loss modeling, we anticipate many other uses for the historical ShakeMap Atlas, including disaster response planning, regional capacity building, and outreach programs.

EXPO-CAT provides an estimate of the number of people exposed to moderate-to-severe levels of ground shaking for earthquakes from January 1973 through December 2007. Population exposures are aggregated into half-intensity unit bins using the LandScan 2006 global population database. We include present day exposure estimates, coupled with our best estimate of exposure hindcast to the date of the earthquake. An online version of EXPO-CAT also incorporates earthquake loss, and other information from PAGER-CAT to streamline loss modeling efforts.

Two examples of the use of EXPO-CAT have been demonstrated: (1) a method to objectively rank country earthquake vulnerability and (2) a quantitative evaluation of the relationship between time-of-day and earthquake mortality rates. Spatial examination of our simple vulnerability rankings indicates that certain countries in different geographical regions appear to cluster spatially according to their relative vulnerability. This provides us with a means to combine our objective rankings with those of expert opinion to formulate more realistic vulnerability rankings where it may be necessary to group countries in order to develop loss models from a combined dataset. In developing these data-driven rankings, it is also worth considering that systematic biases in macroseismic intensity assignments may exist from country-to-country. These country-specific intensity assignments are used to calibrate the ShakeMaps to model the ground-shaking observed for a given earthquake (e.g., Wald et al.

2005). Because we assume equivalence between all intensity scales, and their application, these biases could affect the estimated ShakeMap ground motions, which could subsequently affect the number of people exposed to discrete levels of ground shaking. If significant, biases in population exposure could influence fatality rate estimation methods and vulnerability ranking assessments for a particular country.

Earthquake mortality rates examined herein do not indicate a dominant time-of-day effect, but small correlations may exist. The regional data analyses suggest that the number of people exposed to severe ground shaking appears to be a better indicator of earthquake mortality than time-of-day, with some of the highest exposure quakes occurring during late-night and early-morning hours. Consequently, real-time systems that estimate the number of people exposed to severe ground-shaking, such as PAGER, are of vital importance to alert emergency responders to potential earthquake disasters. However, PAGER population exposure numbers are only as good as the input models and assumptions used to generate them. Uncertainties in ground-motion and population exposure estimation contribute to PAGER uncertainties. Furthermore, loss models developed on these assumptions also rely on historical population numbers estimated from hindcasting present-day population exposures. In this hindcasting approach, we assume a constant, country-specific growth rate for earthquakes back to 1973. We do not account for differences in population growth in rural and urban regions within a country, which are likely to differ given increased global urbanization in the past few decades (e.g., Todaro 1969; Shen and Spence 1996).

Using the full Atlas of ShakeMaps, we merge each of these maps and find the maximum peak ground acceleration observed at any location in the world for the past 35 years. This "composite ShakeMap" is subsequently compared to the 10% in 50 years GSHAP global seismic hazard map. In general, these analyses suggest that existing global, and regional, hazard maps tend to overestimate hazard (i.e., less than 7% exceedance in 35 years from composite ShakeMap; see Table 2), the only exception being Japan. Although the composite ShakeMap is not sufficient to evaluate global hazard itself, it does provide a useful guide as to whether hazard maps, such as GSHAP, offer a realistic interpretation of global seismic hazard in high-exposure, high-risk regions.

The intended use of EXPO-CAT for earthquake loss modeling for the PAGER program is the focus of ongoing research. However, we expect that these data will be useful for other researchers in the earthquake loss arena and will provide a framework for the development of alternative loss methodologies with a systematically derived set of ShakeMap hazard inputs.

Acknowledgments Keith Porter and Kishor Jaiswal are thanked for many discussions that helped outline the development of EXPO-CAT. Vince Quitoriano and Bruce Worden are also thanked for providing ShakeMap development support throughout this work. Reviews of earlier related material and the present paper by Mary Lou Zoback, Jim Dewey, Charles Mueller, Andrew McPherson and Hyeuk Ryu helped improve this manuscript. Comments from two anonymous reviewers also led to valuable improvements to the manuscript. Finite-fault, ground-motion, and intensity constraints used in the ShakeMap Atlas are the aggregated sum of numerous post-earthquake reconnaissance reports, published earthquake studies, and strong-motion monitoring network efforts, all of which help build a comprehensive view of individual events. Citations to these sources are found in Allen et al. (2008). Funding for this research was provided in part by a grant from USAID. Figures 5, 6, and 7 were produced using Generic Mapping Tools (Wessel and Smith 1991).

References

Allen TI, Wald DJ (2009) Evaluation of ground-motion modeling techniques for use in Global ShakeMap: a critique of instrumental ground-motion prediction equations, peak ground motion to macroseismic intensity conversions, and macroseismic intensity predictions in different tectonic settings. US Geological Survey Open-File Report 2009-1047, Golden, CO, 114 p

Allen TI, Wald DJ, Hotovec AJ, Lin K, Earle PS, Marano KD (2008) An Atlas of ShakeMaps for selected global earthquakes. US Geological Survey Open-File Report 2008-1236, Golden, CO, 47 p
Allen TI, Marano KD, Earle PS, Wald DJ (2009) PAGER-CAT: a composite earthquake catalog for calibrating global fatality models. Seismol Res Lett 80(1):57–62. doi:10.1785/gssrl.80.1.57
Bhaduri B, Bright E, Coleman P, Dobson J (2002) LandScan—locating people is what matters. Geoinformatics 5(2):34–37
Bilham R (2004) Urban earthquake fatalities: a safer world, or worse to come? Seismol Res Lett 75:706–712
Building Seismic Safety Council (2004) NEHRP recommended provisions for seismic regulations for new buildings and other structures, 2003 edn. Federal Emergency Management Agency 450, Washington, 338 p
Center for International Earth Science Information Network (2005) Gridded Population of the World Version 3 (GPWv3), Socioeconomic Data and Applications Center (SEDAC), Columbia University, Palisades. http://sedac.ciesin.columbia.edu/gpw. Retrieved 26 March 2009
Coburn AW, Spence RJS, Pomonis A (1992) Factors determining human casualty levels in earthquakes: mortality prediction in building collapse, 10th World Conference Earthquake Engineering, Madrid, pp 5989–5994
Dobson JE, Bright EA, Coleman PR, Durfee RC, Worley BA (2000) LandScan: a global population database for estimating populations at risk. Photogramm Eng Rem S 66(7):849–857
Earle PS, Wald DJ, Allen TI, Jaiswal KS, Porter KA, Hearne MG (2008) Rapid exposure and loss estimates for the May 12, 2008 M_W 7.9 Wenchuan earthquake provided by the US Geological Survey's PAGER system. 14th World Conference of Earthquake Engineering, Beijing, Paper S31-039
Giardini D, Grünthal G, Shedlock KM, Zhang P (1999) The GSHAP global seismic hazard map. Ann Geofis 42(6):1225–1230
Godt J, Şener B, Verdin K, Wald D, Earle P, Harp E, Jibson R (2008) Rapid assessment of earthquake-induced landsliding. Proceedings of the First World Landslide Forum, United Nations University, Tokyo, 4 p
Grünthal G, Bosse C, Sellami S, Mayer-Rosa D, Giardini D (1999) Compilation of the GSHAP regional seismic hazard for Europe, Africa and the Middle East. Ann Geofis 42(6):1215–1223
International Organization for Standardization (2007) Codes for the representation of names of countries and their subdivisions—Part 1: country codes. ISO 3166-1:2006. International Organization for Standardization, Geneva
Jackson J (2006) Fatal attraction: living with earthquakes, the growth of villages into megacities, and earthquake vulnerability in the modern world. Philos Trans R Soc A 364:1911–1925
Jaiswal KS, Wald DJ (2008) Creating a global building inventory for earthquake loss assessment and risk management. US Geological Survey, Open-File Report 2008-1160, Golden, CO, 103 p
Jaiswal KS, Wald DJ, Porter KA (2008) Development of a global, semi-empirical approach for rapid estimation of human casualties due to earthquakes. Seismol Res Lett 79(2):314
Johnson MS (1998) The tale of the tragedy of Neftegorsk. Prehosp Disaster Med 13(1):59–64
Lomnitz C (1970) Casualties and behavior of populations during earthquakes. Bull Seismol Soc Am 60(4):1309–1313
Machette MN, Crone AJ, Bowman JR (1993) Geologic investigations of the 1986 Marryat Creek, Australia earthquake—implications for paleoseismicity in stable continental regions. US Geol Surv Bull, 29 p
Macintyre AG, Barbera JA, Smith ER (2006) Surviving collapsed structure entrapment after earthquakes: a "time-to-rescue" analysis. Prehosp Disaster Med 21(1):4–19
Marano KD, Wald DJ, Allen TI (2009) Global earthquake casualties due to secondary effects: a quantitative analysis for improving PAGER losses. Nat Hazards 49. doi:10.1007/s11069-009-9372-5
McCue K (1999) Seismic hazard mapping in Australia, the southwest Pacific and southeast Asia. Ann Geofis 42(6):1191–1198
Petersen MD, Frankel AD, Harmsen SC, Mueller CS, Haller KM, Wheeler RL, Wesson RL, Zeng Y, Boyd OS, Perkins DM, Luco N, Field EH, Wills CJ, Rukstales KS (2008) Documentation for the 2008 update of the United States National Seismic Hazard Maps. US Geological Survey Open-File Report 2008-1128, 128 p
Porter K, Jaiswal K, Wald D, Earle P, Hearne M (2008a) Fatality models for the US Geological Survey's Prompt Assessment of Global Earthquake for Response (PAGER) system, 14th World Conference of Earthquake Engineering, Beijing, Paper S04-009
Porter KA, Jaiswal KS, Wald DJ, Greene M, Comartin C (2008b) WHE-PAGER Project: a new initiative in estimating global building inventory and its seismic vulnerability, 14th World Conference of Earthquake Engineering, Beijing, Paper S23-016
Radu C, Polonic G, Apopei I (1979) Macroseismic field of the March 4, 1977 Vrancea earthquake. Tectonophys 53:185–186. doi:10.1016/0040-1951(79)90062-3
Ramirez M, Peek-Asa C (2005) Epidemiology of traumatic injuries from earthquakes. Epidemiol Rev 27: 47–55. doi:10.1093/epirev/mxi005

Scawthorn C, Iemura H, Yamada Y (1978) World largest destruction earthquakes since 1900. Sendai, pp 318–319

Shedlock KM, Tanner JG (1999) Seismic hazard map of the western hemisphere. Ann Geofis 42(6): 1199–1214

Shen J, Spence NA (1996) Modelling urban—rural population growth in China. Environ Plan A 28(8): 1417–1444. doi:10.1068/a281417

Spence R (2007) Saving lives in earthquakes: successes and failures in seismic protection since 1960. Bull Earthquake Eng 5:139–251. doi:10.1007/s10518-006-9028-8

The MathWorks (2008) Matlab: the language of technical computing, user guide. The MathWorks, Natick MA

Tierney K, Khazai B, Tobin LT, Krimgold F (2005) Social and public policy issues following the 2003 Bam, Iran, earthquake. Earthq Spectra 21(S1):S513–S534. doi:10.1193/1.2098928

Todaro MP (1969) A model of labor migration and urban unemployment in less developed countries. Am Econ Rev 59(1):138–148

US Geological Survey (2008) Significant earthquakes of the world. http://earthquake.usgs.gov/eqcenter/eqarchives/significant/sig_2008.php. Retrieved 16 June 2008

United Nations (2006) Population growth and distribution. http://unstats.un.org/unsd/demographic/products/indwm/tab1c.htm. Retrieved March 2007

Wald DJ, Allen TI (2007) Topographic slope as a proxy for seismic site conditions and amplification. Bull Seismol Soc Am 97(5):1379–1395. doi:10.1785/0120060267

Wald DJ, Quitoriano V, Heaton TH, Kanamori H (1999a) Relationship between peak ground acceleration, peak ground velocity, and Modified Mercalli Intensity in California. Earthq Spectra 15(3):557–564. doi:10.1193/1.1586058

Wald DJ, Quitoriano V, Heaton TH, Kanamori H, Scrivner CW, Worden BC (1999b) TriNet "ShakeMaps": Rapid generation of peak ground-motion and intensity maps for earthquakes in southern California. Earthq Spectra 15(3):537–556. doi:10.1193/1.1586057

Wald DJ, Worden BC, Quitoriano V, Pankow KL (2005) ShakeMap manual: technical manual, user's guide, and software guide. US Geological Survey, Reston, VA, 132 p

Wald DJ, Earle PS, Allen TI, Jaiswal K, Porter K, Hearne M (2008a). Development of the US Geological Survey's PAGER system (Prompt Assessment of Global Earthquakes for Response), 14th World Conference of Earthquake Engineering, Beijing Paper 10-0008

Wald DJ, Lin K, Quitoriano V (2008b) Quantifying and qualifying ShakeMap uncertainty. US Geological Survey Open-File Report 2008-1238, Golden, CO, 27 p

Wessel P, Smith WHF (1991) Free software helps map and display data. EOS 72:441. doi:10.1029/90EO00319

World Health Organization (2008) Emergency and humanitarian action: China, Sichuan earthquake. http://www.wpro.who.int/NR/exeres/20DF60A7-7A24-4C47-8574-CD0AE3D493D8.htm. Retrieved 8 August, 2008

Zhang P, Yang Z-X, Gupta HK, Bhatia SC, Shedlock KM (1999) Global seismic hazard assessment program (GSHAP) in continental Asia. Ann Geofis 42(6):1167–1190